Positions, lifetimes, and partial widths of metastable quasienergy states by solving the time-dependent complex-scaled Schrödinger equation

Nir Ben-Tal,[a] Nimrod Moiseyev,[a] and Claude Leforestier
Laboratoire de Chimie Théorique, Université de Paris-Sud, 91405 Orsay, France
Ronnie Kosloff
The Fritz Haber Research Center for Molecular Dynamics, The Hebrew University, Jerusalem 91904, Israel

(Received 20 December 1990; accepted 23 January 1991)

The method presented here is based on the solution of the time-dependent complex-scaled Schrödinger equation to provide the complex-scaled evolution operator after one optical cycle. This method is mainly suitable in the study of multiphoton ionization or dissociation under the influence of *high* intense fields. An illustrative numerical example is given.

I. INTRODUCTION

Multiphoton ionization and dissociation of atoms and molecules are currently intensively studied by theoreticians and experimentalists.[1–7] For field intensities above 10^{11} W/cm^2 nonlinear effects predominate in the atomic and molecular systems and nonperturbative approaches should be taken.[8]

Chu and Reinhardt[9,10] calculated the multiphoton ionization rates by extending the Floquet theory to include continuum. The ionization (or dissociation) rates are associated with the imaginary parts of the complex eigenvalues of the truncated time-independent complex-scaled Floquet–Hamiltonian matrix.

To the best of our knowledge, all published works on the multiphoton ionization/dissociation rates by the complex-Floquet theory, were also based on the solution of the time-independent eigenvalue problem

$$\hat{\mathscr{H}}\phi_\alpha = \varepsilon_\alpha \phi_\alpha\,, \tag{1}$$

where

$$\mathscr{H}_{n,m} = -\frac{1}{2}\nabla^2 e^{-2i\theta} + \frac{1}{T}\int_0^T V(e^{i\theta}\mathrm{x},t')\,dt' + \hbar\omega n\,,$$

$$\mathscr{H}_{n,n'\neq n} = \frac{1}{T}\int_0^T V(\mathrm{x}e^{i\theta},t')\exp[i\omega(n'-n)t']\,dt'\,, \tag{2}$$

and

$$T = \frac{2\pi}{\omega} \tag{3}$$

is the time periodicity of the Hamiltonian and ω is the frequency of the time-dependent field.

The complex eigenvalues provide the positions and widths of the metastable quasienergy states

$$\varepsilon_\alpha = E_\alpha(\text{position}) - \frac{i}{2}\Gamma_\alpha(\text{width}) \tag{4}$$

and

$$\tau_\alpha(\text{lifetime}) = \hbar/\Gamma_\alpha\,. \tag{5}$$

For an infinite large Floquet matrix $\mathscr{H}$, the quasienergies are assigned an additional good quantum number n. Such that

$$\varepsilon_\alpha = \varepsilon_{\alpha'} + \hbar\omega n, \tag{6}$$

where $\varepsilon_{\alpha'}$ are associated with a single Brillouin zone (e.g., $n = 0$ channel). Resulting of the truncation of $\mathscr{H}$ there is an "edge effect" which makes it hard to isolate the quasienergies which are associated with a single Brillouin zone. This difficulty becomes a severe one as the intensity of the field gets a high value and many channels (i.e., Brillouin zones) are involved in the dissociation/ionization process. In such a case there is a need to diagonalize a very large Hamiltonian matrix since the dimension of $\mathscr{H}$ in the variational calculations, is equal to the product of the number of channels (i.e., number of terms in the Fourier series expansion of the quasienergy state) and the number of basis functions which are taken into consideration. No doubt that when not too many channels are involved in the dissociation/ionization process, this method is efficient and useful.[11] However, we found it less efficient and hard to use when there are many resonance quasienergy states in a single Brillouin zone and also when the intensity of the field is high.

The purpose of this work is to show that resonance positions, widths, and partial widths of metastable quasienergy states can be obtained from solutions of the time-dependent Schrödinger equation over the first optical cycle. The method proposed here is based on previous works where the Floquet theory was used, without complex scaling, in the study of laser-driven dissociative systems (see, e.g., Hirschfelder, Wyatt, and co-workers)[12] and on the work of Leforestier and Wyatt who studied the solutions of the complex-symmetric Floquet–Hamiltonian.[13] The first step of the calculation is to construct a complex-evolution matrix $\mathrm{U}(0|T)$ by solving the complex-scaled time-dependent Schrödinger equation. The complex eigenvalues of $\mathrm{U}(0|T)$, λ_α, are associated with the quasienergies of the studied time-periodic Hamiltonian. So far the procedure is very similar to the one used before, for example, by Leforestier and Wyatt.[13] However, as we shall show in Sec. II, the effect of the complex

---

[a] Permanent address: Department of Chemistry, Technion—Israel Institute of Technology, Haifa 32000, Israel.

scaling on the results is large. As in the time-independent cases, the continuum states can be distinguished from the resonance states. The continuum solutions form a spiral in the complex λ plane. One edge of the spiral is $0 + i0$ and the other one is $1 + i0$ if the threshold energy of the bare Hamiltonian is taken as zero. The resonance solutions are stable and not much affected by varying θ [remember that $\exp(i\theta)$ is the complex scaling factor]. The resonance widths are given by

$$\Gamma_\alpha = -2\,\mathrm{Im}\left[\frac{i\hbar}{T}\log\lambda_\alpha\right] \tag{7}$$

and the resonance positions (modulo $\hbar\omega$) of the quasienergy states are

$$\varepsilon_\alpha = \mathrm{Re}\left[\frac{i\hbar}{T}\log\lambda_\alpha\right]. \tag{8}$$

The key step in the calculation is the computation of the complex-scaled evolution operator U. Basically two types of procedures can be used. In the first one, the column vectors of U are propagated in time one by one to a given desired accuracy. In the second type of procedures, the entire matrix U is propagated in time to keep exactly the same numerical error in the evolution of each one of the vectors in the evolution matrix U. Several different possible computational methods for the computation of U are described and compared in Sec. III.

The probability for ionization or dissociation resulting from absorbing n photons can be approximately estimated from the ratio between the partial widths Γ_n (defined to be a factor of the residue of the S matrix at a pole) and the total width Γ_α. The partial widths were previously obtained for time-independent Hamiltonians (including the Floquet–Hamiltonian matrix) by the asymptotic analysis of the complex-scaled resonance states.[14–17]

In our case the calculation of the partial widths is less straightforward as one can see in Sec. IV. A summary of the method proposed here is given in Sec. V.

As an illustrative numerical example we studied the simple case where

$$\hat{H} = -\frac{1}{2}\frac{d^2}{dx^2} + f(x)[1 + a\cos(\omega t)] \tag{9}$$

and chose $f(x)$ to be the Rosen–Morse potential[18]

$$f(x) = -\frac{V_0}{\cos h^2(\alpha x)}, \tag{10}$$

since it does not support resonances when t is treated adiabatically and since it has been used before as a testbed for theories and computational methods.[11]

In our calculations we chose $V_0 = 2$, $\alpha = 1/\sqrt{3}$; then $f(x)$ supports three bound states at the energies $-\frac{3}{2}$, $-\frac{2}{3}$, and $-\frac{1}{6}$. (For the resonance positions, widths, and partial widths as function of a, see Ref. 11.)

II. RESONANCE POSITIONS AND WIDTHS (LIFETIMES) OF QUASIENERGY STATES

The solution of the time-dependent Schrödinger equation

$$\hat{H}(\mathbf{x},t)\Psi(\mathbf{x},t) = i\hbar\frac{d\psi(\mathbf{x},t)}{dt} \tag{11}$$

can be given by

$$\Psi(\mathbf{x},t) = \hat{U}(\mathbf{x},t)\Psi(\mathbf{x},0), \tag{12}$$

where $\hat{U}(\mathbf{x},t)$ is the time evolution operator. For time-periodic Hamiltonians following the Floquet–Bloch theorem, there are quasistationary solutions Ψ_α for which

$$\Psi_\alpha(\mathbf{x},t) = e^{-i\varepsilon_\alpha t/\hbar}\Phi_\alpha(\mathbf{x},t) \tag{13}$$

and

$$\Phi_\alpha(\mathbf{x},t) = \Phi_\alpha(\mathbf{x},t+T). \tag{14}$$

By substituting Eqs. (13) and (14) into Eq. (12) one immediately can see that by solving the eigenvalue problem

$$\hat{U}(\mathbf{x},T)\phi_\alpha(\mathbf{x},T) = \lambda_\alpha\Phi_\alpha(\mathbf{x},T) \tag{15}$$

the quasienergies mapped to a single Brillouin zone are obtained

$$\lambda_\alpha = \exp(-i\varepsilon_\alpha T/\hbar). \tag{16}$$

For metastable systems the resonance quasistationary solutions $\Phi_\alpha(\mathbf{x},t)$ exponentially diverge as $\mathbf{x}\to\infty$. However, they become square integrable functions upon complex scaling.[9–11] We may suggest (on the basis of our numerical experience) to carry out the following transformation:

$$\mathbf{x}\to(\mathbf{x}-\mathbf{x}_0)\exp(i\theta) + \mathbf{x}_0, \tag{17}$$

where $\mathbf{x}_0$ is the vector position at the minimum of the field-free potential. Consequently, the complex eigenvalues of the complex-scaled time-evolution operator are associated with complex-quasi-"energy" solutions ε_α. When $\hat{H}(\mathbf{x},t)$—[from now on $\mathbf{x}$ stands for a complex-scaled coordinate, $\mathbf{x} = (\mathbf{x}' - \mathbf{x}_0)\exp(i\theta) + \mathbf{x}_0$]—can be written as

$$\hat{H} = \hat{H}_0(\mathbf{x}) + \hat{H}_1(\mathbf{x},t). \tag{18}$$

Then, instead of solving the differential Eqs. (11) and (12), one can use the eigenfunctions of the complex-scaled $\hat{H}_0$ as a basis set,

$$\hat{H}_0\Psi_i^{(0)} = E_i^{(0)}\Psi_i^{(0)}$$

and solve the following time-dependent matrix problem:

$$\mathscr{H}\mathrm{U}(0|t) = i\hbar\frac{d\,\mathbf{U}(0|t)}{dt}, \quad t\varepsilon[o,T], \tag{19}$$

where

$$\mathbf{U}(0|0) = \mathbf{1} \tag{20}$$

and

$$\mathscr{H}_{ij}(t) = E_i^{(0)}\delta_{ij} + \langle\Psi_i^{(0)}|\hat{H}_1(\mathbf{x},t)|\Psi_j^{(0)}\rangle. \tag{21}$$

For the different computational methods to evaluate $\mathrm{U}(0|T)$ see Sec. III. The complex-quasienergies ε_α are associated with the eigenvalues of the complex matrix $\mathrm{U}(T)$,

$$\mathrm{U}(0|T)\mathbf{D}_\alpha = \lambda_\alpha\mathbf{D}_\alpha, \tag{22}$$

as defined in Eq. (16). The complex eigenvalues λ_α can be divided into two different sets. The first one is of the resonances which are the complex (i.e., $|\lambda_\alpha| < 1$) eigenvalues that are θ independent. The second type of complex eigenvalues are θ dependent and are associated with the rotating continua. Following the Balslev and Combes theorem

$$\varepsilon_\alpha(\text{continuum}) = (\tilde{\varepsilon}_\alpha + \hbar\omega n)\exp(-2i\theta) - \hbar\omega n\,;$$
$$\tilde{\varepsilon}_\alpha \epsilon [-\hbar\omega n, \infty]\,, \qquad (23)$$

where

$$n = -\infty, ..., \infty.$$

Here we assume (without loss of generality) that the thershold energy of the bare (i.e., field free) Hamiltonian is zero. By substituting Eq. (23) into Eq. (16) one can see that

$$\lambda_\alpha(\text{continuum}) = e^{-i[\cos 2\theta \cdot (\tilde{\varepsilon}_\alpha + \hbar\omega n) - \hbar\omega n]T/\hbar}$$
$$\times e^{-(\tilde{\varepsilon}_\alpha + \hbar\omega n)T\sin 2\theta/\hbar}, \qquad (24)$$

where

$$n = -\infty, ..., \infty.$$

Therefore, the second class of solutions which are associated with the rotating continua in a *single* Brillouin zone will form a spiral in the complex λ plane. The edge of the spiral will be at $\lambda_\alpha = 1 + i\,0$ (i.e., $\tilde{\varepsilon}_\alpha = -\hbar\omega n$), whereas the core of the spiral is at $\lambda_\alpha = 0 + i\,0$ ($\tilde{\varepsilon}_\alpha = \infty$).

Indeed, the results for the Rosen–Morse time-dependent model Hamiltonian (described in Sec. I) which are presented in Fig. 1 confirm this analysis.

As we can see from Fig. 1 [and also from Eq. (24)] the spiral has a fractal dimensionality and the rate of convergence to the origin of $\lambda_\alpha = 0$, strongly depends on the value of the rotational angle θ. [$\exp(i\theta)$ is the complex scaling factor.] Consequently, the resonances will be more easily distinguished from the continuum solutions as θ becomes larger.

The fact that the resonances can be easily isolated from the continuum is shown in Fig. 2. A basis set of 50 eigenvectors of complex-scaled field-free Hamiltonian matrix $\hat{H}_0$ (those which were associated with the lowest real parts of $E_i^{(0)}$) were used. From Fig. 2 one can see that most of the eigenvalues of U(0|T) (39 out of 50) fall into the core of the spiral. The resonances and rotating continua are affected by the strength intensity of the field a.

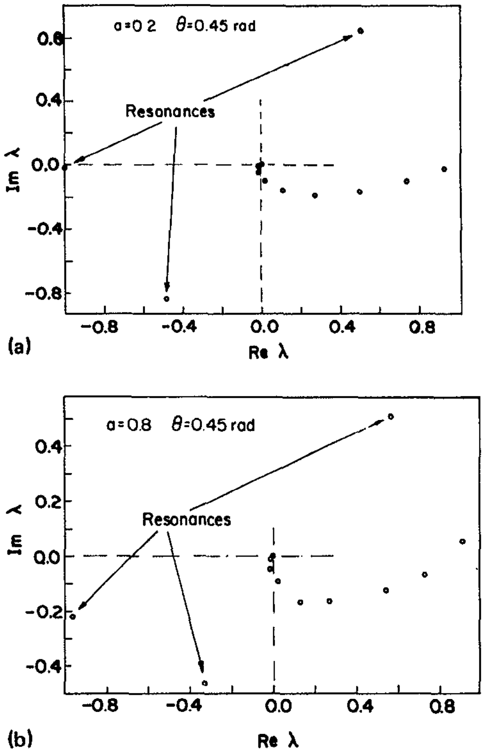

FIG. 2. The resonance and scattering eigenvalues of the time evolution matrix after one optical cycle U(0|T) using 50 particle in a box basis functions. (a) Weak field intensity of $a = 0.2$. (b) Strong field intensity of $a = 0.8$.

We may stress here that there is not a simple unique procedure to find out in which Brillouin zone a given quasienergy is located. (See, however, a possible way to allocate the Brillouin zones in Sec. IV). This fact is clearly illustrated in Fig. 3 where the complex quasienergies $\varepsilon_\alpha = i\hbar \log \lambda_\alpha / T$ are shown in the complex-ε_α plane.

Identification of the Brillouin zone in which a given quasienergy state is located will provide the familiar Balslev–Combes behavior of resonances and rotating continuum as were obtained by solving the time-independent Floquet–Hamiltonian (see Fig. 2 in Ref. 11).

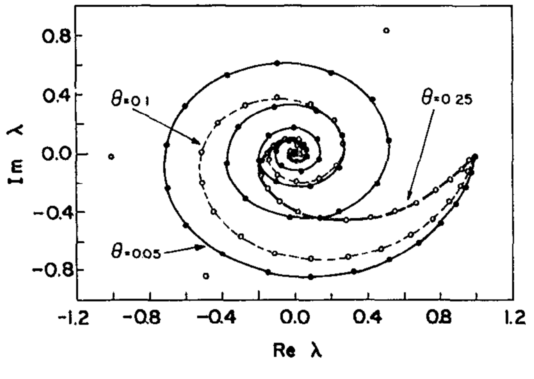

FIG. 1. Complex eigenvalues $\{\lambda_i\}$ of the first optical cycle complex-scaled evolution matrix U(0|T) for the time-periodic Rosen–Morse Hamiltonian [Eq. (9)] with the field intensity $a = 0.2$ and $T = 2\pi$. The three isolated open circles stand for the resonance eigenvalues which are not affected by the value of the rotational angle θ.

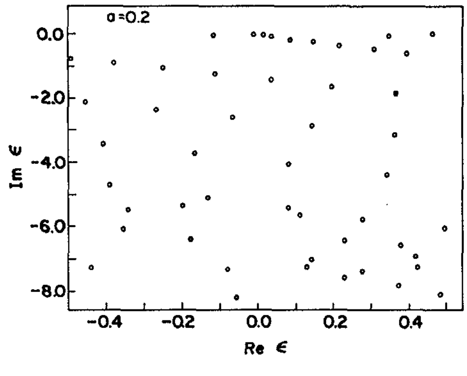

FIG. 3. Complex quasienergies in one Brillouin zone (not necessarily the same one), $\varepsilon = (i\hbar/T)\ln \lambda_\alpha$, obtained for the Rosen–Morse time periodic Hamiltonian [Eq. (9)].

III. THE COMPLEX–SCALED EVOLUTION OPERATOR BY DIFFERENT COMPUTATIONAL METHODS

As was described before, the resonance positions and widths can be obtained by propagating the evolution operator $\hat{U}$ for one optical cycle provided complex scaling has been carried out. Roughly the procedure can be divided in two: (1) constructing a faithful representation of the Hilbert space of the problem; (2) propagating the evolution operator $\hat{U}$.

(1) In representing the Hilbert space a few alternatives have been tried. The first is a basis set expansion. The most simple of these expansions is the particle in a box basis set. Other basis sets are possible, such as the harmonic oscillator basis set. The restriction on the choice of basis sets is the ability to apply the complex scaling since the dilation of the Hamiltonian is equivalent to the scaling of the basis functions by a complex factor,

$$\mathscr{H}_{ij}(t) = \int_{-\infty}^{\infty} \phi_i^*(\mathbf{x}')\hat{H}(\mathbf{x}'e^{+i\theta},t)\phi_j(\mathbf{x}')\,d\mathbf{x}'$$

$$= \int_{-\infty}^{\infty} [\phi_i(\mathbf{x}'e^{+i\theta})]^*\hat{H}(\mathbf{x}',t)\phi_j(\mathbf{x}'e^{-i\theta})\,d\mathbf{x}' . \tag{25}$$

For cases in which the applied field is not too strong, the use of the interaction picture can produce a much smaller basis set. The interaction representation is produced by prediagonalizing $\hat{H}_0$, the time-independent part of the Hamiltonian matrix H. The alternative to the basis set expansion is the use of a discrete variable representation (DVR).[19] The natural choice, in analogy to the particle in the box representation, is the Fourier representation. The basic idea is a dual discrete representation, both in configuration space and, via the fast Fourier transform (FFT), also in momentum space[20] and is to perform the operation of an operator in Hilbert space on a vector locally. For the potential operation a configuration representation leads to the operation

$$\mathbf{V}(x_i e^{i\theta};t)\psi(x_i) \tag{26}$$

on all the grid points x_i. The potential operation can be applied directly to the operator $\hat{U}$ which was discretized as

$$\mathbf{U}(x_i,x_j';t) . \tag{27}$$

The kinetic energy operation is local in momentum representation. A forward FFT transforms the vector to momentum space. The kinetic energy operation becomes

$$\frac{k^2}{2m}e^{-2i\theta} . \tag{28}$$

The operation is completed by an inverse Fourier transform back to configuration space. The procedure can be generalized to the operation on the operator $\hat{U}$. The operator $\hat{U}$ is transformed to momentum space by a mixed forward (on x_m) and backward (on x_n') Fourier transform.

$$U_{k_j,k_l,t} = \iint \langle k_j|x\rangle\langle x|\hat{U}(t)|x'\rangle\langle x'|k_l\rangle\,dx\,dx' \tag{29}$$

and the discrete version

$$U_{(k_j,k_l,t)} = \frac{1}{2\pi N}\sum_{m=0}^{N-1}\sum_{n=0}^{N-1} U(x_m,x_n';t)\exp[2\pi i(ln-jm)/N] .$$

Two advantages can be identified in the Fourier method: (a) the complex-scaling procedure, $\mathbf{x}\rightarrow\exp(i\theta)\mathbf{x}$, is direct and can be applied to all coordinates simultaneously; (b) the matrix operations scale as $\sim N\log N$ compare to $\sim N^2$ of matrix multiplication. This means that for very large basis sets the Fourier method will be always advantageous.

(2) Considering the propagation scheme: The equation of motion for the time-evolution operator $\hat{U}$ given in a matrix representation becomes

$$i\hbar\frac{d\mathbf{U}}{dt} = \mathscr{H}(t)\mathbf{U} . \tag{30}$$

The solution is complicated by the explicit time dependence of the Hamiltonian. Basically two methods have been tried.

The first method propagates each vector in the initial evolution operator separately for one optical cycle by means of the Adams–Moulton predictor–corrector method[21]

$$i\hbar\frac{d\mathbf{U}_n(0|t)}{dt} = \mathscr{H}(t)\mathbf{U}_n(0|t) , \quad n = 1,2,\ldots,N,$$

$$U_{m,n}(0|0) = \delta_{m,n} , \tag{31}$$

where the time-evolution matrix over the first optical cycle $\mathbf{U}(0|T)$ is given by

$$\mathbf{U}(0|T) = [(\mathbf{U}_1(0|T),\mathbf{U}_2(0|T),\ldots,\mathbf{U}_N(0|T)] . \tag{32}$$

The advantage of this method is that in situations without strong mixing some vectors may require less numerical effort than others. The propagation method used in this work is the sixth order Adams–Moulton predictor–corrector variable time step,[22] which provides a prediction to the seventh time-grid point of $\mathbf{U}_n$ based on the previous calculated sixth time-grid points of $\mathbf{U}_n$. Insertion of the predicted seventh time-grid point of $\mathbf{U}_n$ to the time-dependent Schrödinger equation provides the time derivative of $\mathbf{U}_n$ which is needed in the calculation of the desired corrector. Previous experience[13] has shown that this method can provide the Floquet eigenvalues as accurate as are needed, when the imaginary component of the complex quasienergy is much smaller than the real one (i.e., for narrow resonances).

The alternative to propagating the vectors of $\mathbf{U}$ one by one is to propagate them simultaneously. The idea is to break up the total propagation to many small time steps Δt,

$$\hat{U}(0|t) \simeq \prod_n \hat{U}(t_n|t_n+\Delta t) . \tag{33}$$

It is assumed that within each interval the variation of $\hat{H}$ is small such that a short time solution can be obtained by a truncated Magnus series

$$\hat{U}(t_n|t_n+\Delta t)$$

$$\simeq \exp\left(-\frac{i}{\hbar}\int_{t_n}^{t_n+\Delta t}\hat{H}(t')\,dt' - \frac{1}{2\hbar^2}\int_{t_n}^{t_n+\Delta t}\left\{\int_{t_n}^{t'}[\hat{H}(t'),\hat{H}(t'')]\,dt''\right\}dt' + \cdots\right) . \tag{34}$$

We are left now with the problem of exponentiating the operator $\hat{H}$. The most simple solution is to use a Taylor expansion. An expansion of five to ten terms has been tried. There are two sources of error, one is the truncation of the Magnus series and the other is the truncation of the Taylor expansion. These two errors should be balanced. In our case only a convergence in the lower right quarter of the complex energy plane $\mathscr{D}$ is required. That is, $\mathrm{Re}(E) > E_{\text{threshold}}$ and $\mathrm{Im}(E) < 0$. Therefore, the Taylor series expansion is not an optimal one since any point in the complex energy plane which is located *inside* a circle centered at $[\mathrm{Re}(E) = E_{\text{threshold}}, \mathrm{Im}(E) = 0]$ is converged.

An alternative to the Taylor series expansion is to use a uniform polynomial expansion. This is a generalization to the complex plane of the Chebychev polynomial which is uniform in the interval $(-1,1)$.[23] The advantage of a uniform approximation is that all the vectors in **U** are propagated with the same error. The uniform interpolation points on the boundary of $\mathscr{D}$ can be obtained by making use of the Schwartz–Cristoffel transformation which maps the evenly distributed interpolation points on the boundary of a circle in the complex energy plane into the boundary of the domain $\mathscr{D}$. Once the interpolating points $\{z_0, z_1, z_2, \ldots\}$ are known, then the interpolating polynomial can be obtained. For numerical stability the polynomial is presented in Newton's form[24]

$$f(z) \simeq P(z) = a_0 + a_1(z - z_0) + a_2(z - z_1)(z - z_0) + \cdots , \qquad (35)$$

where the coefficients can be recursively obtained

$$a_0 = f(z_0), \quad a_1 = \frac{f(z_0) - f(z)}{z_0 - z}, \ldots .$$

The polynomial approximation in Eq. (35) is applied to the exponential function of Eq. (34) where z is replaced by the truncated Magnus series.

The three methods mentioned above, (A) sixth order Adams–Moulton prediction corrector; (B) second order Magnus series expansion combined with the Taylor expansion and the FFT; and (C) second order Magnus series expansion combined with the uniform polynomial expansion obtained by the Schwartz–Cristofel mapping algorithm, were applied to the complex-scaled Rosen–Morse time-periodic Hamiltonian. The results presented in Table I show three resonance complex eigenvalues of the time-evolution operator after one optical cycle [see Eq. (15)],

$$\lambda_\alpha = \rho_\alpha \exp(i\gamma_\alpha), \qquad (36)$$

obtained by the methods (A), (B), and (C). By far the most rapid convergence was obtained by method (A), where each vector in the initial time evolution operator was separately propagated for one optical cycle. However, different results may be obtained for other cases. The slightly different results obtained for the two broad resonances are due to accumulated roundoff error.

IV. PARTIAL WIDTHS OF MULTIPHOTON DISSOCIATION (IONIZATION) PROCESS

The partial widths are defined to be factors of the residues of the S matrix at a pole. In a half-collision process the ratio between the partial width Γ_n and the total width provide the probability for dissociation or ionization resulting of absorbing n photons. The partial widths for time-periodic Hamiltonians were previously obtained by Moiseyev, Bench, and Korsch[17] exactly as it was first proposed for time-independent Hamiltonians by Peskin, Moiseyev, and Lefebvre.[14]

The resonance complex-quasienergy state has been expanded in a Fourier series

$$\Psi_{\text{res}} = e^{-i\varepsilon_{\text{res}}T/\hbar}\Phi_{\text{res}}(x,t), \qquad (37)$$

$$\Phi_{\text{res}}(x,t) = \sum_{n=-\infty}^{\infty} \phi_n^{\text{res}}(x)\, e^{i\omega n t}, \qquad (38)$$

where ε_α is the complex quasienergy of the resonance which is allocated in the first Brillouin zone (i.e., $n = 0$). If n is an open channel for dissociation (ionization) and the threshold energies of the field-free Floquet Hamiltonian is $E_t = -\hbar\omega n$, then the complex scaled $\phi_n^{\text{res}}(x)$ takes the asymptotic form

$$\phi_n^{\text{res}}(x) \to a_n \left[\frac{\mu}{\hbar k_n}\right]^{1/2} \exp[ik_n x \exp(i\theta)], \qquad (39)$$

where

$$k_n = [2\mu(\varepsilon_{\text{res}} - \hbar\omega n)]^{1/2}/\hbar. \qquad (40)$$

The partial widths are given by[14]

$$\Gamma_n = \hbar|a_n|^2. \qquad (41)$$

More recently a new formula for the partial widths was derived by Moiseyev and Peskin from the complex resonance-scattering theory [see Eq. (19) in Ref. (16)],

$$\Gamma_n = \left|\frac{\hbar^2}{2\mu}\lim_{x\to\infty} W[f_n, \phi_n]\right|^2, \qquad (42)$$

where W stands for the Wronskian

TABLE I. The three resonance eigenvalues of the time-evolution operator after one optical cycle, $\lambda_\alpha = \rho_\alpha \exp(i\gamma_\alpha)$, obtained by the methods (A), (B), and (C) described in Sec. III for the time periodic Rosen–Morse Hamiltonian.

Methods	ρ_1	γ_1	ρ_2	γ_2	ρ_3	γ_3
(A)	0.994 066 1	3.364 645	0.5685	4.0909	0.757	0.728
(B)	0.994 066 4	3.364 645	0.5685	4.0910	0.758	0.730
(C)	0.994 065 4	3.364 653	0.5688	4.0915	0.758	0.729

$$W[f,g]=f\frac{dg}{dx}-g\frac{df}{dx} \tag{43}$$

and

$$f_n=\sqrt{\frac{\mu}{\hbar k_n}}\exp(-ik_nxe^{i\theta}) \tag{44}$$

or, in the radial case ($x\varepsilon[0,\infty]$),

$$f_n=-2i\sqrt{\frac{\mu}{\hbar k_n}}\sin(k_nxe^{i\theta})\,. \tag{45}$$

This formula provided stable partial widths in the study of HD/Ag(111) resonances. We shall show here its applicability and numerical stability (lack of oscillations) in the calculation of the partial widths of the time-period Rosen–Morse model Hamiltonian.

The main difficulty in calculating the partial widths by the methods described in Secs. II and III is due to the following facts:

(1) We do not get directly the Fourier components of $\Phi(x,t)$. However, the Fourier component and $\Phi(x,t)$ can be easily computed.

(2) The eigenfunctions of the time-evolution operator $\mathbf{U}(0|T)$ provide $\Phi(x,T)$ (i.e., after one optical cycle only) and *not* Φ at any given time.

(3) All of the quasienergy states obtained by the diagonalization of $\mathbf{U}(0|T)$ are located in a single Brillouin zone, but *not* necessarily in the same one (e.g., see Fig. 3).

Let us assume that $\lambda_{\rm res}$ and $\mathbf{D}_{\rm res}$ are the complex eigenvalue and eigenvector of $\mathbf{U}(0|T)$ which are associated with a resonance state. In order to get the desired Fourier transform components we first need to calculate $\Phi_{\rm res}(x,t)$ in the time interval $t\varepsilon[0,T]$. We shall use the periodicity property of $\Phi_{\rm res}$ by solving once more the time-dependent Schrödinger equation

$$\mathscr{H}(t_j)\mathbf{D}(t_j)=i\hbar\frac{d\mathbf{D}(t_j)}{dt},\quad j=0,1,\ldots,\frac{T}{\Delta t}-1\,, \tag{46}$$

where

$$\mathbf{D}(0)=\mathbf{D}_{\rm res}, \tag{47}$$

$$t_j=j\Delta t\,, \tag{48}$$

and $T/\Delta t$ should be an even number. The time-dependent periodic complex-scaled function $\Psi_{\rm res}(x,t_j)$ is now given by

$$\Psi_{\rm res}(x,t_j)=\sum_{i=1}^{N}D_i^{\rm res}(t_j)\psi_i^{(0)}\,. \tag{49}$$

$\Psi_i^{(0)}$ are the variational known eigenfunctions of the complex-scaled field-free Hamiltonian H_0.

In the next step of the calculations we carry out a Fourier transform of $\mathbf{D}_{\rm res}(k\Delta t)$; $k=0,1,\ldots$. The results of the Fourier transform of the components of the vector $\mathbf{D}_{\rm res}$ are stored in a matrix $A_{i,k}$ where $i=1,2,\ldots,N$ and the index k is associated with the $n=[(T/2\Delta t)-k]$ Fourier component. The components ϕ_n in the Fourier series expansion of $\Phi_\alpha(x,t)$ are now available

$$\phi_n(x)=\sum_{i=1}^{n}A_{i,n}\psi_i^{(0)}(\mathbf{x}) \tag{50}$$

and

$$\Psi_\alpha(x,k\Delta t)=\lambda_\alpha^{k\Delta t/T}\sum_{n=1-T/2\Delta t}^{T/2\Delta T}\phi_n(x)e^{+i\omega nk\Delta t}\,. \tag{51}$$

Before carrying out the asymptotic analysis of ϕ_n, we should identify the Brillouin zone in which each one of the resonance quasieneregy states is localized. Let n_α denote the Brillouin zone in which ψ_α is localized. n_α is the value of n for which

$$\left|\sum_{i=1}^{N}A_{i,n}^2\right|^2 \tag{52}$$

gets a maximal value. Now we can shift the indices in the Fourier series expansion of ψ_α to localize the resonance quasienergy states at the same (zero) Brillouin zone

$$\begin{aligned}E_{\rm res}^{\alpha}&=\frac{i\hbar}{T}\log\lambda_\alpha-h\omega n_\alpha\\&=\varepsilon_\alpha(\text{position})-\frac{i}{2}\Gamma(\text{width})\,,\end{aligned} \tag{53}$$

$$\tilde\phi_{-n}(\mathbf{x})=\phi_{n_\alpha-n}(x)\,,$$

where $n=1,2,3,\ldots$.

The partial widths Γ_n can be obtained from the asymptotic analysis of $\tilde\phi_n$. Two formulas are given[14–16]

$$\Gamma_n(x)=\hbar\left|\sqrt{\frac{\hbar k_n}{\mu}}\,e^{-ik_nx}\tilde\phi_{-n}(\mathbf{x})\right|^2 \tag{54}$$

and

$$\Gamma_n(x)=\frac{1}{\hbar}\left|\frac{\hbar^2}{2\mu}W[f_n,\tilde\phi_{-n}]\right|^2, \tag{55}$$

where

$$\begin{aligned}&x=(x'-x_0)\,e^{i\theta}+x_0\,,\\&(\hbar k_n)^2/2\mu=E_{\rm res}-\hbar\omega n\,,\end{aligned} \tag{56}$$

and x' is a real variable. $\Gamma_n(x)$ is the "local" width in contrast to the partial width $\Gamma_n=\lim_{x\to\infty}\Gamma_n(x)$ which is θ independent. The partial widths satisfy the condition

$$\Gamma_\alpha\equiv-2\,{\rm Im}(E_{\rm res})=\sum_{n=1}\Gamma_n \tag{57}$$

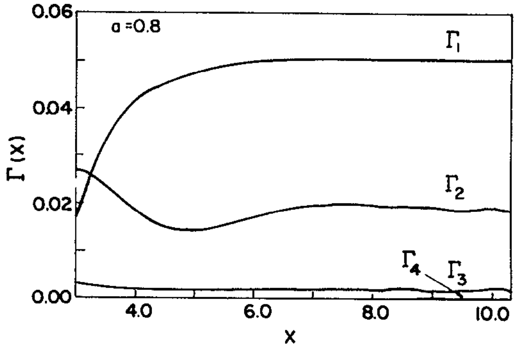

FIG. 4. Partial widths $\Gamma_n=\lim_{x\to\infty}\Gamma_n(x)$ for four channels opened for dissociation obtained by the asymptotic analysis of the ($\tilde\varepsilon_\alpha=-0.6512+\hbar\omega n$, $\Gamma_{\rm total}/2=0.071$) resonance wave function which is associated with the first excited state of the field-free Rosen–Morse Hamiltonian.

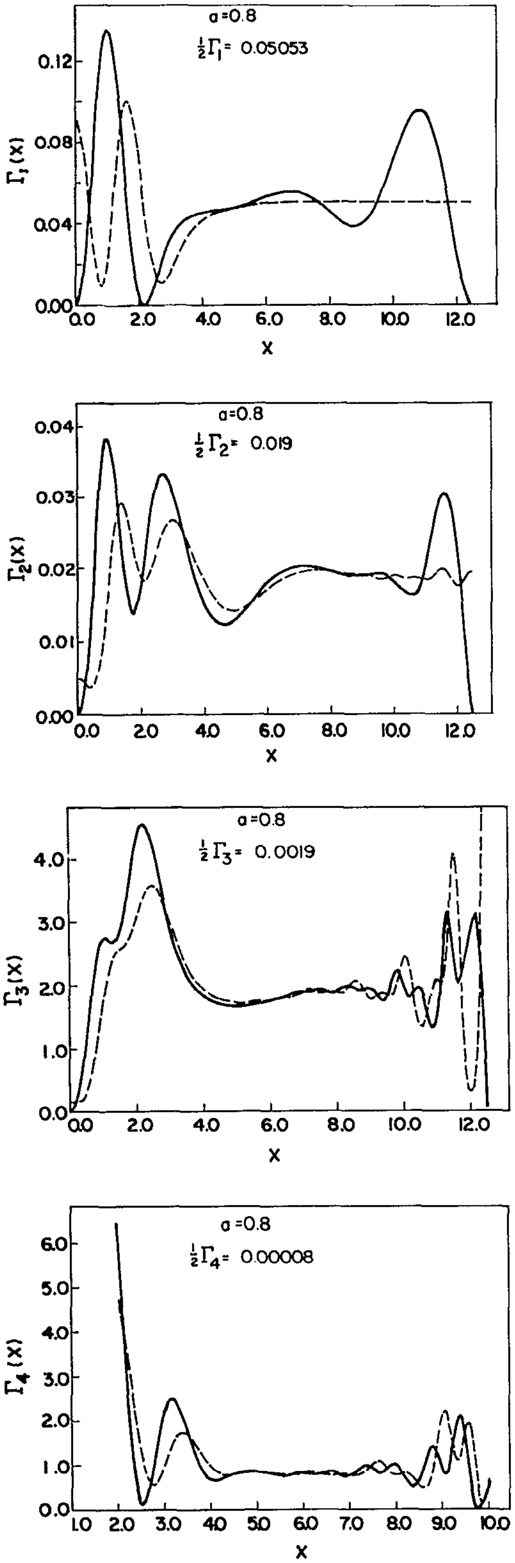

FIG. 5. A comparison between partial widths Γ_n, $n = 1,2,3,4$ obtained by the asymptotic analysis of the complex-scaled resonance quasienergy states by the two different formulas given in Eq. (54) (solid line) and in Eq. (55) (dashed line).

whereas Γ_n/Γ_α provides the probability of ionization or dissociation due to the absorption of n photons by the atomic or molecular systems.

The results presented in Fig. 4 were obtained by using Eq. (55) in the analysis of the Rosen–Morse quasienergy states.

The partial widths Γ_n are estimated from the plateau obtained as $\Gamma_n(x)$ is varied with x. The use of formula (55) rather than Eq. (54) increases dramatically the stabilization length of the plateau and also reduces the amplitude of the oscillations obtained near the edge of the box (see Fig. 5).

V. SUMMARY

For a time-periodic Hamiltonian given by

$$\hat{H} = \hat{H}_0(\mathbf{x}) + \hat{H}_1(\mathbf{x},t),$$

where

$$\hat{H}_1(\mathbf{x},t+T) = \hat{H}_1(\mathbf{x},t),$$

the positions and widths (inverse lifetimes) of the metastable quasienergy states can be calculated as follows:

(1) Complex scale the internal coodinates of the Hamiltonian $\mathbf{x} \rightarrow (\mathbf{x} - \mathbf{x}_0)\exp(i\theta) + \mathbf{x}_0$, where $\mathbf{x}_0$ is the vector position at the minimum of the field-free potential V_0.

(2) Calculate the "first" n eigenfunctions $\Psi_i^{(0)}$ of the complex-scaled $\hat{H}_0$. That is, the eigenfunctions which are associated with the n-lowest real parts of $E_i^{(0)}$, where $E_i^{(0)}$ are the complex eigenvalues of $\hat{H}_0$. Note that $\psi_i^{(0)}$ can be calculated on m grid points or can be constructed of m-basis functions ($m \geqslant n$).

(3) Use the field-free Hamiltonian eigenfunctions $\psi_i^{(0)}$ to construct the $n \times n$ matrix $\mathscr{H}_1$.

(4) Solve the time-dependent Schrödinger equation to get the evolution matrix $\mathbf{U}(0|T)$ [see Eqs. (19)–(21)]. $\mathbf{U}(0|T)$ can be obtained by propagating the entire unitary matrix $\mathbf{U}(0|0) = 1$, or by propagating the column vectors of $\mathbf{U}$ one by one as described in Sec. III.

(5) Calculate the complex eigenvalues λ_α of $\mathbf{U}(0|T)$. Vary the value of θ. The θ-independent solutions are the resonances. The resonance positions (modulo $\hbar\omega$) $\varepsilon_{\rm res}$ and widths $\Gamma_{\rm res}$ are obtained from Eqs. (7) and (8). The continuum solutions appear as a spiral in the complex λ plane.

The probability for ionization/dissociation and the partial widths can be obtained as follows:

(6) Calculate the eigenvector of $\mathbf{U}(0|T)$, $\mathbf{D}_{\rm res}$, which is associated with the resonance eigenvalue $\lambda_{\rm res}$.

(7) Solve the time-dependent Schrödinger equation $\mathscr{H}(t)\,\mathbf{D}_{\rm res}(t) = i\hbar d\,\mathbf{D}_{\rm res}(t)/dt$, where $t\epsilon[0,T]$ (see discussion in Sec. IV). Store the time dependent solutions every Δt time steps.

(8) Carry out a Fourier transform of $\mathbf{D}_{\rm res}(k\Delta t)$; $k = 0,1,...,[(T/\Delta t) - 1]$. Store the results of the Fourier transform in a matrix $\mathbf{A}$.

(9) Use $\mathbf{A}$ to construct the coefficients $\Phi_n(\mathbf{x})$ in Fourier series expansion of the resonance quasienergy state as given in Eqs. (50).

(10) Find the optical cycle (Brillouin zone) $n_{\rm res}$ at which the resonance quasienergy state $\psi_{\rm res}$ is mostly localized [see Eq. (52)].

(11) Shift the indexes of $\Phi_n(\mathbf{x})$ [obtained in step (9) of the calculations] to localize $\Psi_{\rm res}$ at the zero Brillouin zone [see Eqs. (53)].

(12) Calculate the partial widths Γ_n from the asymptotic analysis of $\tilde{\Phi}$ [see Eqs. (54)–(56)]. $\Gamma_n/\Gamma_{\text{res}}$ provides the probability for ionization or dissociation resulting from absorbing n photons.

ACKNOWLEDGMENT

This work was done while one of the authors (N.M.) was holding an Invited Prefessorship from Université de Paris-Sud, Orsay, France.

[1] F. H. M. Faisal, *Theory of Multiphoton Processes* (Plenum, New York, 1987).
[2] N. B. Delone and V. P. Krainov, *Atoms in Strong Laser Fields* (Springer, Berlin, 1985).
[3] V. S. Letokhov, *Non-linear Laser Chemistry*, Springer Series in Chemical Physics, Vol. 22 (Springer, Berlin, 1983).
[4] M. M. Mittleman, *Introduction to the Theory of Laser–Atom Interaction* (Plenum, New York, 1982).
[5] D. S. King, Adv. Chem. Phys. **50**, 105 (1982).
[6] M. Qhack, Adv. Chem. Phys. **50**, 395 (1982).
[7] N. Bloembergen and E. Yablonovitch, Phys. Today **31**, 23 (1978).
[8] Z. Deng and J. H. Eberly, J. Opt. Soc. Am. B **2**, 486 (1985).
[9] S.-I. Chu and W. P. Reinhardt, Phys. Rev. Lett. **39**, 1195 (1977).
[10] S.-I. Chu, Adv. At. Mol. Phys. **21**, 197 (1985).
[11] N. Moiseyev and H. J. Korsch, Phys. Rev. A **41**, 493 (1990); Isr. J. Chem. **30**, 107 (1990), and references therein.
[12] D. R. Dion and J. O. Hirschfelder, Adv. Chem. Phys. **35**, 265 (1976); P. K. Aravind and J. O. Hirschfelder, J. Phys. Chem. **88**, 4788 (1984); S. C. Leasure, and K. F. Milfeld, Phys. Rev. A **27**, 72 (1983); C. Leforestier and R. E. Wyatt, *ibid.* **25**, 1250 (1982).
[13] C. Leforestier and R. E. Wyatt, Chem. Phys. **98**, 123 (1985).
[14] U. Peskin, N. Moiseyev, and R. Lefebvre, J. Chem. Phys. **92**, 2902 (1990).
[15] R. Lefebvre and N. Moiseyev, Chem. Phys. Lett. **163**, 339 (1989).
[16] N. Moiseyev and U. Peskin, Phys. Rev. A **42**, 255 (1990).
[17] N. Moiseyev, F. Bench, and J. Korsch, Phys. Rev. A **42**, 4045 (1990).
[18] N. Rosen and P. N. Morse, Phys. Rev. **42**, 210 (1932); L. D. Landue and E.M. Lifshitz, *Quantum Mechanics* (Pergamon, New York, 1965), p. 72.
[19] J. V. Lill, G. A. Parker, and J. C. Light, Chem. Phys. Lett. **89**, 483 (1982); J. C. Light, I. P. Hamilton, and J. V. Lill, J. Chem. Phys. **82**, 1400 (1985); J. P. Hamilton and J. C. Light, *ibid.* **84**, 306 (1986); Z. Bačic and J. C. Light, *ibid.* **85**, 4594 (1986); **86**, 3065 (1987).
[20] D. Kosloff and R. Kosloff, J. Comput. Phys. **52**, 35 (1983); M. D. Feit, J. A. Fleck, and A. J. Steiger, Am. J. Comput. Phys. **47**, 412 (1982).
[21] P. Henrici, *Discrete Variable Methods in Ordinary Differential Equations* (Wiley, New York, 1962), pp. 194–202.
[22] W. H. Press, B. P. Flannery, S. A. Tenkoliky, and W. T. Venerling, *Numerical Recipes* (Cambridge University, Cambridge, 1988), pp. 569–572.
[23] R. Kosloff, J. Phys. Chem. **92**, 2087 (1988); H. Tal Ezer and R. Kosloff, J. Chem. Phys. **81**, 3967 (1984).
[24] M. Berman, R. Kosloff, and H. Tal-Ezer, J. Phys. A (submitted).